

ANALYTICAL AND EXPERIMENTAL STUDIES ON FATIGUE CRACK PATH UNDER COMPLEX MULTIAXIAL LOADING

M. de Freitas, B. Li e L. Reis

Department of Mechanical Engineering
Instituto Superior Técnico, Av. Rovisco Pais, 1049-001, Portugal

Resumo. Em componentes e estruturas de engenharia ocorrem falhas devido a carregamentos adicionais e por vezes inesperados, como por exemplo carregamentos de flexão e torção por falta de alinhamento, etc. A análise fractográfica da superfície de fractura assim como a orientação da fenda ajudam a identificar os efeitos produzidos por um determinado carregamento. Existem vários factores que influenciam a trajectória da fenda de fadiga, tais como o material, a geometria do componente, a trajectória do carregamento, etc. O objectivo do artigo é estudar a influência de diferentes trajectórias de carregamento multiaxial na orientação da fenda de fadiga. Realizaram-se ensaios numa máquina servo-hidráulica biaxial em provetes de aço 42CrMo4, com trajectórias de carregamento biaxial diferentes. Realizou-se a análise fractográfica do plano de iniciação da fenda. Foi também feita a previsão teórica dos planos de dano críticos através do uso de critérios: Brown-Miller, Findley, Wang-Brown, Fatemi-Socie, SWT e Liu. A comparação entre os resultados obtidos experimentalmente e previstos pelos critérios mostra que os modelos de fadiga multiaxial ao corte dão uma boa estimativa.

Abstract. In real engineering components and structures, many accidental failures were due to unexpected or additional loadings, such as additional bending or torsion, etc. Fractographical analyses of the failure surface and the crack orientation are helpful for identifying the effects of the non-proportional multiaxial loading. There are many factors influencing the fatigue crack paths, such as the material type, structural shape and loading path, etc. This paper studies the effects of multiaxial loading path on the crack path. Experiments were conducted on a biaxial testing machine, on the specimen made of steel 42CrMo4, with six different biaxial loading paths. Fractographical analyses of the plane of crack initiation and propagation were carried out. Theoretical predictions of the damage plane were conducted using the Brown-Miller, the Findley, the Wang-Brown, the Fatemi-Socie, the SWT and the Liu's criteria. Comparisons of the predicted orientation of the damage plane with the experimental observations show that the shear-based multiaxial fatigue models give very good predictions.

1. INTRODUCTION

In structural durability analyses, the prediction of the potential crack path as well as fatigue lifetime is very important for safety evaluations and failure mode analyses. In a critical component or structure, the crack path can determine whether fatigue failure is benign or catastrophic. Besides, the knowledge of potential crack paths is also important for the selection of appropriate non-destructive testing procedures and structural design for crack arrest. Therefore, the study on the crack paths has received increasing attentions in the recent years.

In real engineering structures, there are many factors influencing the fatigue crack paths, such as the material type (microstructure), structural geometry and loading path, etc. It is widely believed that fatigue crack nucleation and growth are caused by cyclic plasticity. Forsyth [1] has designated two stages of crack growth, stage I where cracks grow along the planes of maximum shear stress and stage II where cracks grow on the plane normal to the direction of the maximum principal stress. Kanazawa et al [2] studied the endurance and the direction of crack growth of 1Cr-Mo-V steel under out-of-phase axial/torsional loading

conditions, significant influences of the out-of-phase loading conditions were shown. The crack paths have been paid increasing attention in the field of multiaxial fatigue as reviewed by Socie and Marquis [3].

The objective of this paper is to study the effects of non-proportional loading paths on the fatigue crack paths of the material 42CrMo4 steel. Various fatigue models are applied and evaluated for correlating the crack orientations. In the experimental studies, six loading cases are tested and the crack plane orientation are analysed by optical microscope. In this study, only the orientations of crack nucleation and early growth were investigated, which correspond to the stage I crack growth according to Forsyth [1].

The influence of the loading paths on the crack orientation was observed. Then the multiaxial fatigue models, such as the critical plane models and also the energy-based critical plane models, are applied for predicting the orientation of the critical plane. The predictions are compared with experimental and observations. The applicability of the multiaxial models is discussed for the material and loading paths studied.

2. MATERIAL DATA, SPECIMEN FORM AND TEST PROCEDURE

The material studied in this paper is the high strength steel 42CrMo4. The chemical composition and monotonic mechanical properties are shown in Tables 1 and 2, respectively.

Table 1. Chemical composition of the material studied 42CrMo4 (in wt%)

C	Si	Mn	P	Cr	Ni	Mo	Cu
0.39	0.17	0.77	0.025	1.10	0.30	0.16	0.21

Table 2. Monotonic mechanical properties of the material studied

Tensile strength	R_m (MPa)	1100
Yield strength	$R_{p0.2, \text{monotonic}}$ (MPa)	980
Elongation	A (%)	16
Young's modulus	E (GPa)	206
Hardness	HV	362

The geometry and dimensions of the specimen are shown in Figure 1.

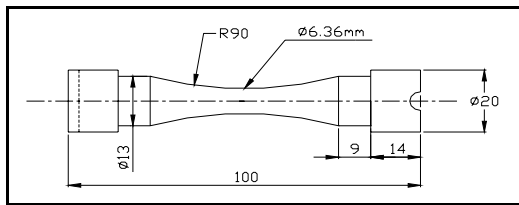


Figure 1. Specimen geometry for biaxial cyclic tension-compression with cyclic torsion tests

In order to characterize the cyclic stress-strain behaviour of the materials studied, tension-compression low cycle fatigue tests were carried out using a biaxial servo-hydraulic machine. The cyclic properties obtained by fitting the test results are shown in Table 3.

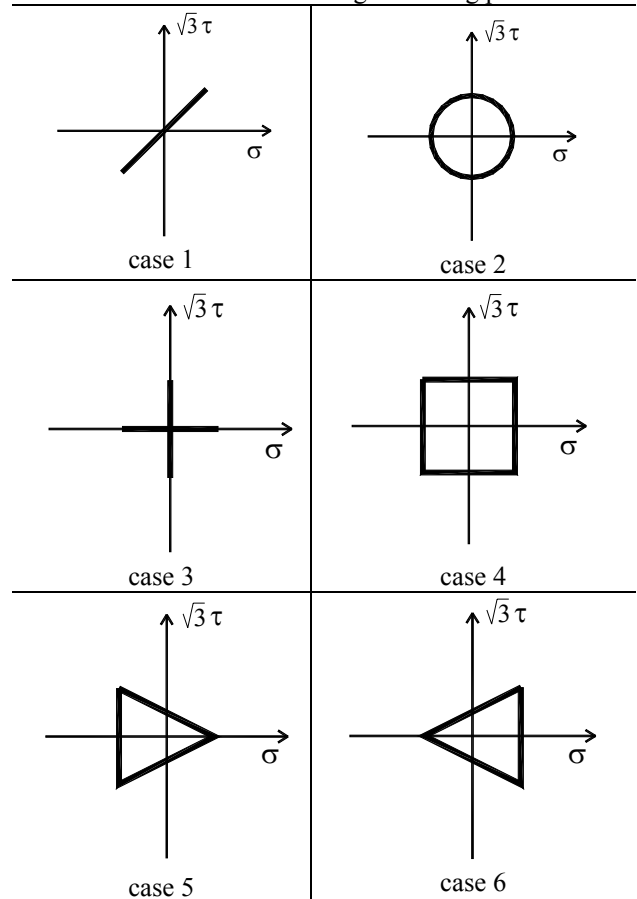
Table 3: Cyclic properties of 42CrMo4 steel ($f=0.2s^{-1}$)

Yield strength	$R_{p0.2, \text{cyclic}}$ (MPa)	540
Strength coefficient	K' (MPa)	1420
Strain hardening exponent	n'	0.12
Fatigue strength coefficient	σ_f' (MPa)	1154
Fatigue strength exponent ^b		-0.061
Fatigue ductility coefficient	ϵ_f'	0.18
Fatigue ductility exponent	c	-0.53

To study the effects of the multiaxial loading paths on the fatigue crack paths, a series of loading paths were

applied in the experiments as shown in Table 4. The tests of biaxial cyclic tension-compression with cyclic torsion were performed by a biaxial servo-hydraulic machine. Test conditions were as follows: frequency 4-6 Hz at room temperature and laboratory air. Tests ended up when the specimens were completely broken. Then, fractographic analysis of the macroscopic plane of crack initiation and early crack growth were carried out, using an optical microscope at a magnification between 10 and 100 times. Some of the specimens were also analysed in the SEM microscope. The measurement of the crack initiation plane orientation was carried out as follows: firstly, the crack initiation was identified, as indicated by a white arrow on the left side in Figure 2; then, the specimen was analysed in a 3D measurement device and the angle between the crack initiation plane and the longitudinal axis was accurately measured, as shown on the right side of Figure 2. This procedure and one example for each loading path are shown in figure 2. Experimental measured angle planes are presented in Table 5.

Table 4. Multiaxial fatigue loading paths



3. THEORETICAL ANALYSES OF THE FATIGUE CRACK PLANES

For the six biaxial loading cases shown in Table 4, the potential crack plane orientation is analysed by various critical plane models and energy-based critical plane model, such as the Brown-Miller, the Findley, the

Wang-Brown, the Fatemi-Socie, the SWT and the Liu's criteria.

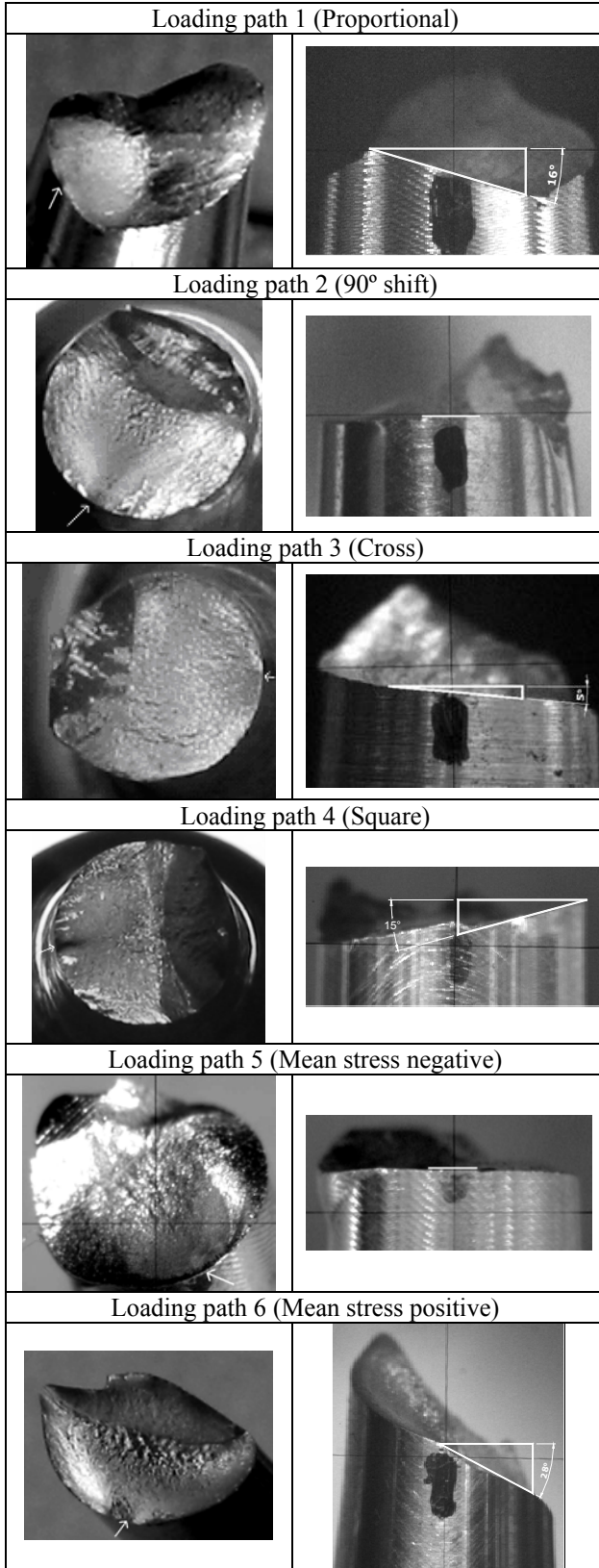


Figure 2. Fractographic analyses of the fatigue failure plane orientations for each of the six loading paths in Table 4.

Brown-Miller Model

According to Brown-Miller criterion [4], the critical plane is defined as the plane where the shear strain amplitude has maximum value:

$$\max_{\theta} \left(\frac{\Delta\gamma}{2} \right) \quad (1)$$

where $\Delta\gamma$ is the shear strain range on a plane θ . Figure 3 shows the variations of the Brown and Miller parameter on different plane orientation θ , under the six loading cases. For each loading case, the plane angle with the maximum Brown-Miller parameter can be identified and they are summarized in Table 5.

Findley Model

Based on physical observations of the orientation of initial fatigue cracks in steel and aluminium, Findley [5] discussed the influence of normal stress acting on the maximum shear stress plane. A critical plane model was introduced, which predicts that the fatigue crack plane is the plane orientation θ with maximum Findley damage parameter:

$$\max_{\theta} (\tau_a + k\sigma_{n,\max}) \quad (2)$$

where τ_a is the shear stress amplitude on a plane θ , $\sigma_{n,\max}$ is the maximum normal stress on that plane and k is constant material. Figure 4 shows the variations of the Findley parameter on the different plane θ , under the six loading cases. For each loading case, the plane angle with the maximum Findley parameter can be identified and they are summarized in Table 5.

Wang -Brown Model

Based on the Brown-Miller criterion [4], Wang and Brown [6] model defined the critical plane as:

$$\max_{\theta} \left(\frac{\Delta\gamma}{2} + S\Delta\epsilon_n \right) \quad (3)$$

where $\Delta\gamma$ is the shear strain range on a plane θ , $\Delta\epsilon_n$ is the range of normal strain on the same plane θ and S is a material constant. Figure 5 shows the variations of the Wang and Brown parameter on different plane θ , under the six loading cases. For each loading case, the plane angle with the maximum Wang and Brown parameter can be identified and they are summarized in Table 5.

Fatemi-Socie Model

The Fatemi-Socie model [7] predicts the critical plane as the plane orientation θ with the maximum F-S damage parameter:

$$\max_{\theta} \left[\frac{\Delta\gamma}{2} \left(1 + k \frac{\sigma_{n,\max}}{\sigma_y} \right) \right] \quad (4)$$

where $\Delta\gamma/2$ is the maximum shear strain amplitude on a plane θ , $\sigma_{n,\max}$ is the maximum normal stress on that plane, σ_y is the material monotonic yield strength; k is a material constant, which can be found by fitting fatigue data from simple uniaxial tests to fatigue data from simple torsion tests.

Application of the Fatemi-Socie model for the six loading cases show the variations of the F-S parameter on different plane orientations as presented in Fig. 6. For each loading case, the plane angle θ with the maximum F-S parameter can be identified and they are summarized in Table 5.

S-W-T Model

The tensile damage model, proposed by Smith, Watson and Topper [8], predicts that the fatigue crack plane is the plane orientation θ with maximum normal stress (the maximum principal stress):

$$\max_{\theta}(\sigma_n) \frac{\Delta\epsilon_1}{2} \quad (5)$$

where σ_n is the normal stress on a plane θ , ϵ_1 is the normal strain on that plane.

Figure 7 shows the variations of the normal stress σ_n on the different plane θ , under the six loading cases. For each loading case, the plane angle with the maximum normal stress σ_n can be identified and they are summarized in Table 5.

Liu's Virtual Strain-Energy Model

The Liu's virtual strain energy model, VSE, [9] is an energy-based critical plane model. This model considers two possible failure modes: a mode for tensile failure, ΔW_I , and a mode for shear failure, ΔW_{II} . Failure is expected to occur on the plane θ in the material having the maximum VSE quantity.

ΔW_I is computed by firstly identifying the plane on which the axial work is maximized and then adding the respective shear work on that plane:

$$\Delta W_I = (\Delta\sigma_n \Delta\epsilon_n) \max_{\theta} + (\Delta\tau \Delta\gamma) \quad (6)$$

Similarly, ΔW_{II} is computed by firstly identifying the plane on which the shear work is maximized and then adding the axial work on that same plane:

$$\Delta W_{II} = (\Delta\sigma_n \Delta\epsilon_n) + (\Delta\tau \Delta\gamma) \max_{\theta} \quad (7)$$

where $\Delta\tau$ and $\Delta\gamma$ are the shear stress range and shear strain range, respectively, $\Delta\sigma_n$ and $\Delta\epsilon_n$ are the normal stress range and normal strain range, respectively.

Application of the Liu's model for the six loading cases show the variations of the Virtual Strain Energy on different plane orientations as presented in Figure 8 for ΔW_I and Figure 9 for ΔW_{II} . For each loading case, the plane angle θ with the maximum ΔW_I and ΔW_{II} parameters can be identified and they are summarized in Table 5.

4. COMPARISONS BETWEEN EXPERIMENTS AND PREDICTIONS

The predictions of the crack orientations by the multiaxial fatigue models are compared with the experimental observations in Table 5. For the orientations of crack nucleation and early growth investigated in this paper, the shear-based models (Brown-Miller, Findley, Wang-Brown, Fatemi-Socie and Liu II) give better predictions than the tensile-based models (SWT and Liu I). Among the shear-based models, the criteria which define the critical plane as the plane with maximum damage parameter instead of maximum shear strain (stress) amplitude give better predictions. Findley's criterion gives the best prediction, with the maximum deviation of 6° for the square loading path.

5. CONCLUSIONS

A wide range of fatigue loading paths were applied to a quenched and tempered alloy steel (42CrMo4). The initiation crack plane, observed and measured by microscope, is influenced by the loading paths. For the studied material, the shear-based multiaxial models (Findley, Wang-Brown, Fatemi-Socie and Liu II) give very good predictions of the orientation of the crack initiation plane. The comparison between these shear-based models and the crack plane observed and measured were quite accurate.

ACKNOWLEDGEMENTS

Financial support from the Fundação para Ciência e Tecnologia (FCT) is acknowledged.

REFERENCES

1. Forsyth, P.J.E. (1961) *Proceedings of Crack Propagation Symposium*, Cranfield, pp. 76-94.
2. Kanazawa, K., Miller, K. J. & Brown, M.W. (1977) *J. of Engin. Mater. & Technology*, Trans. ASME, **99**(3): 222-228.
3. Socie, D.F. and Marquis, G.B., "Multiaxial Fatigue", Society of Automotive Engineers, Warrendale, PA, (2000).
4. Brown, M.W. and Miller, K.J. (1973) *Proc. of the Inst. of Mechanical Engineers*, **187**, pp. 745-755.
5. Findley, W.N. (1959) *Journal of Engineering for Industry*, pp. 301-306.
6. Wang, C.H. and Brown, M.W. (1996) *J. of Engin. Mater. & Technology*, **118**, pp. 367-370.
7. Fatemi, A. and Socie, D. (1988) *Fatigue and Fracture of Engineering Materials and Structures*, **11**(3), pp. 149-165.
8. Smith, R.N., Watson, P. and Topper, T.H. (1970) *J. of Materials*, **5**(4), pp. 767-778.
9. Liu, K.C. (1993) *Advances in Multiaxial Fatigue*, ASTM STP 1191, D.L. McDowell and R. Ellis, eds., pp. 67-84.

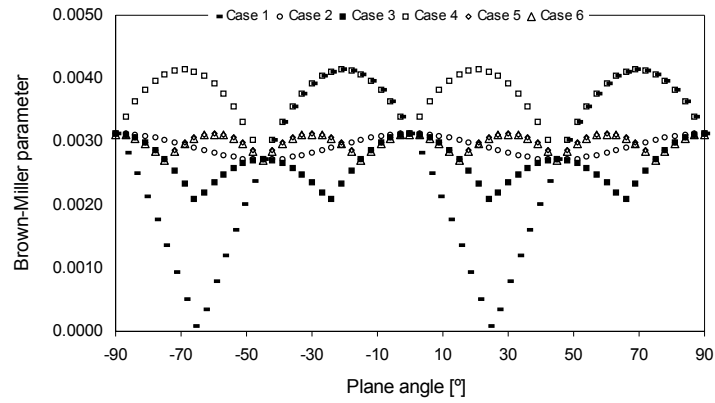


Figure 3. Variations of the shear strain amplitude (B-M parameter) on different plane.

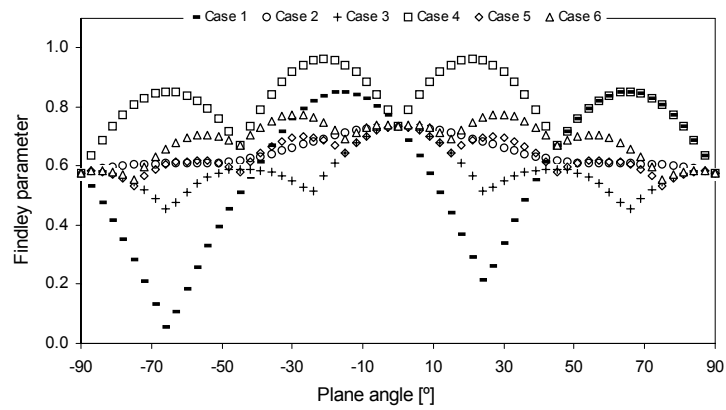


Figure 4. Variations of the Findley parameter on different plane.

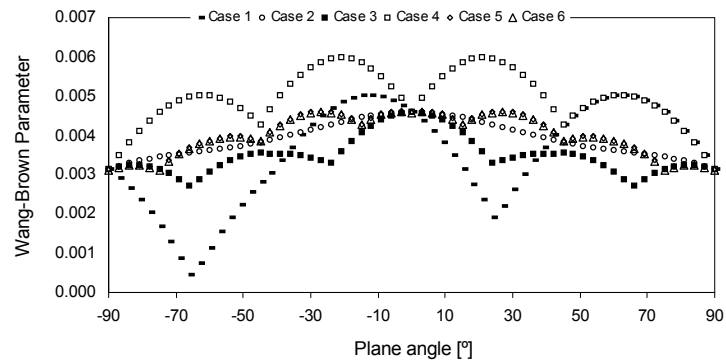


Figure 5. Variations of the Wang-Brown parameter on different plane.

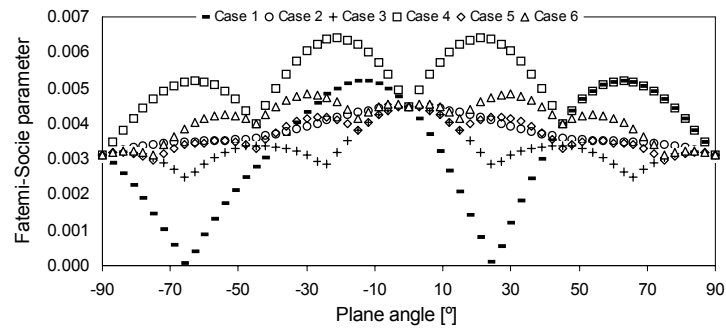


Figure 6. Variations of the Fatemi-Socie parameter on different plane.

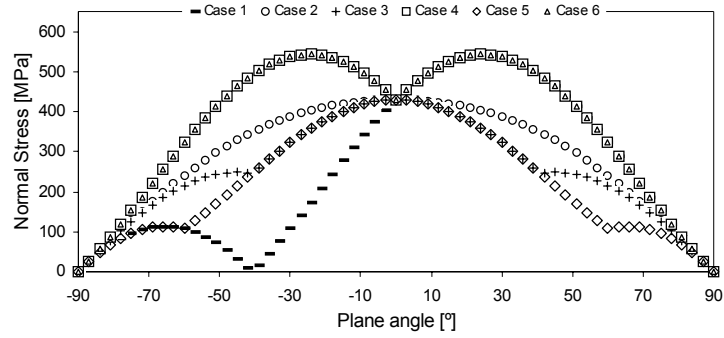


Figure 7. Variations of the S-W-T parameter on different plane.

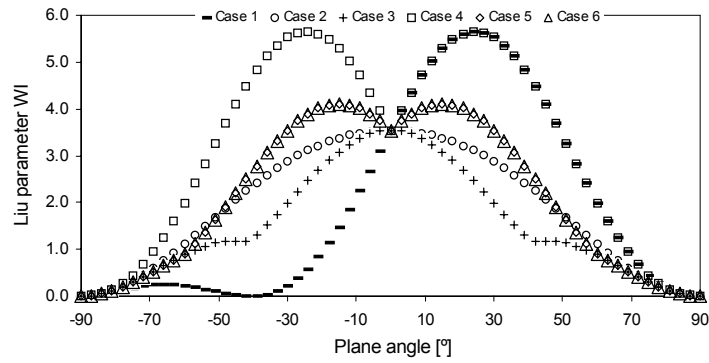


Figure 8. Variations of the Liu W_I parameter on different plane.

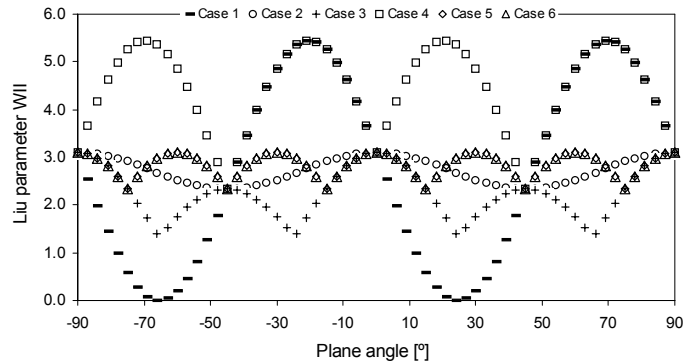


Figure 9. Variations of the Liu W_{II} parameter on different plane.

Table 5. Comparison of the observed crack plane with predictions

	Multiaxial Loading Paths					
	Case 1	Case 2	Case 3	Case 4	Case 5	Case 6
Crack plane observed	-16°	0°	-5°	15°	0°	-28°
<i>Brown-Miller</i>	-21°/69°	0°/±90°	0°/±90°	±21°/±69°	0°/±30°	±30°/0°
<i>Findley</i>	-16°/65°	0°	0°	±21°	0°	±29°
<i>Wang-Brown</i>	-14°/63°	0°	0°	±21°	±3°/±27°	±27°/±3°
<i>Fatemi-Socie</i>	-14°/63°	0°	0°	±21°	0°	±29°
<i>S-W-T</i>	25°	0°	0°	±25°	0°	±25°
<i>Liu I</i>	25°	0°	0°	±25°	±15°	±15°
<i>Liu II</i>	-21°/69°	0°/±90°	0°/±90°	±21°/±69°	0°/±30°	±30°/0°